

Catalysis Science & Technology

Accepted Manuscript



This is an *Accepted Manuscript*, which has been through the Royal Society of Chemistry peer review process and has been accepted for publication.

Accepted Manuscripts are published online shortly after acceptance, before technical editing, formatting and proof reading. Using this free service, authors can make their results available to the community, in citable form, before we publish the edited article. We will replace this *Accepted Manuscript* with the edited and formatted *Advance Article* as soon as it is available.

You can find more information about *Accepted Manuscripts* in the [Information for Authors](#).

Please note that technical editing may introduce minor changes to the text and/or graphics, which may alter content. The journal's standard [Terms & Conditions](#) and the [Ethical guidelines](#) still apply. In no event shall the Royal Society of Chemistry be held responsible for any errors or omissions in this *Accepted Manuscript* or any consequences arising from the use of any information it contains.



Catalysis Science & Technology

Paper

La-modified mesoporous Mg-Al mixed oxides: Effective and stable base catalysts for the synthesis of dimethyl carbonate from methyl carbamate and methanol

Received 00th October 2015,
Accepted 00th January 20xx

DOI: 10.1039/x0xx00000x

www.rsc.org/

Dengfeng Wang,^a Xuelan Zhang,^{*ab} Jie Ma,^{*a} Haiwen Yu,^a Jingzhu Shen^a and Wei Wei^b

A series of La-containing Mg-Al hydrotalcite-like (HTI) precursors with different La content ($\text{Mg}^{2+}:\text{Al}^{3+}:\text{La}^{3+} = 3:1:x$, x from 0 to 1.0) were synthesized using a co-precipitation method followed by hydrothermal treatment. X-ray diffraction and thermogravimetric measurements demonstrated that the yield of the HTI phase decreased with increased La content. The La-modified Mg-Al mixed oxides (HTC-La) were then obtained by thermal decomposition of the corresponding HTI precursors and the mesoporous structure was formed during calcination. It was demonstrated that the structure and surface basic property of the HTC-La samples strongly depended on the amount of La additive. Simultaneously, the resulting HTC-La materials were used as solid base catalysts for the synthesis of dimethyl carbonate (DMC) from methyl carbamate (MC) and methanol. Then, the correlation between their basic properties and catalytic performance was studied in detail. The incorporation of a suitable amount of La into HTC-La catalysts was beneficial for the production of DMC, and a DMC yield of 54.3% with a high DMC selectivity of 80.9% could be achieved when x was tuned to 0.5 under the optimized reaction conditions. In addition, the HTC-La catalyst could be readily recycled while maintaining high catalytic activity and selectivity of DMC. Furthermore, *in situ* FTIR experiments were carried out to elucidate the adsorption behaviours of reactants. On the basis of the experimental results, a plausible basic catalytic mechanism that MC and methanol were activated simultaneously on the basic sites of catalyst was proposed for this catalytic reaction.

1. Introduction

Recently, much effort has been devoted to the development of new synthesis methods based on CO_2 as a feedstock for organic carbonates owing to their excellent properties and commercial applications. As an important homologue of the dialkyl carbonate family, dimethyl carbonate (DMC) has been received much interest. As an environmentally benign building block, DMC can replace phosgene, dimethyl sulphate, chloromethane, and methyl chloroformate as carbonylation, methylation, esterification, or ester interchange reagent for organic synthesis without pollution. DMC is also used as green solvent and flavoring agent of foodstuff due to its low toxicity. More important, it is extensively applied as an oxygen-containing fuel additive in place of toxic and less biodegradable MTBE additives. Moreover, DMC has been used as an electrolyte due to its high dielectric constant.¹⁻⁴ Up to now, a number of synthetic processes are known for the production of DMC including the phosgenation of methanol,

the oxidation carbonation of methanol, and transesterification of organic carbonates. However, each of the aforementioned process suffers from the corresponding shortcomings such as being poisonous, being easily explosive, high investment and production costs.⁵⁻⁷ Recently, CO_2 , a readily available, inexpensive and environmentally acceptable material, has been used as raw material for the DMC synthesis. Nevertheless, the direct synthesis of DMC from CO_2 and methanol is still far from practical application because of the difficulty in activation of carbon dioxide, reactivation of the catalyst and thermodynamic limitation.⁸⁻¹⁰ In order to overcome these shortcomings, an alternative approach is to prepare DMC from urea and methanol, which is widely considered as indirect route for utilization CO_2 because the released NH_3 can be easily separated, recycled and further utilized to produce urea by reaction with CO_2 . Besides, no water is formed during this process.¹¹ Therefore, the subsequent separation and purification would be simple and the cost could be reduced markedly. It is well known that urea methanolysis is a typical stepwise reaction: urea firstly reacts with methanol to produce the intermediate methyl carbamate (MC), which is further converted to DMC by reaction with methanol. It is generally accepted that the first step is fast and highly selective even without catalysts, but the DMC synthesis from MC and methanol is more difficult.^{12,13} Hence, the second reaction is usually considered to be the rate-control step and dividing this process into two isolated steps would be a more

^a College of Chemistry, Chemical Engineering and Materials Science, Zaozhuang University, Zaozhuang, 277160, P.R. China.

^b State Key Laboratory of Coal Conversion, Institute of Coal Chemistry, Chinese Academy of Sciences, Taiyuan, 030001, P.R.China.

Electronic Supplementary Information (ESI) available: [details of any supplementary information available should be included here]. See DOI: 10.1039/x0xx00000x

promising method. Therefore, the key to improve the DMC synthesis via methanolysis of urea is to develop effective catalysts towards the reaction of MC and methanol.

Several kinds of catalysts including organic tin, inorganic salts, ionic liquids, pure metal oxides and Fe₂O₃ supported catalyst have been tested towards the direct reaction of urea and methanol or its analogues.¹⁴⁻¹⁸ Among them, zinc-containing catalysts such as ZnO, Zn-Ce, Zn-Ca and Zn-Al mixed oxides presented high catalytic activity.¹⁹⁻²² Especially, ZnO-CeO₂-La₂O₃ could improve DMC synthesis remarkably and give 50.4% DMC yield.²³ However, the main problem associated with zinc-containing catalysts might be the easy leaching of active component, which has been proved by several researchers. For instance, Zhao *et al.* reported that ZnO was converted to the homogeneous species when it catalyzed urea alcoholysis.²⁴ An *et al.* discovered that ZnO phase of ZnO-PbO catalyst got leached out seriously when it promoted the reaction of ethyl carbamate and ethanol.²⁵ Recently, Fujita and his co-workers further pointed out that synthesis of glycerol carbonate from urea glycerolysis using Zn-containing solid catalysts took place homogeneously but not heterogeneously.²⁶ With respect to the isolated second reaction, solid bases were tested in a batch reactor, but the DMC yield was below 20%.¹² Our group reported that using ZnCl₂ and LaCl₃ as catalysts, the DMC yield could reach 33.6% and 53.7%, respectively.²⁷⁻²⁹ However, it is famous that the catalyst recovery is a great inconvenience for industry production using homogeneous catalyst. In order to develop heterogeneous catalysts, we have found Zn-Fe mixed oxide gave 30.7% of DMC yield.³⁰ Unfortunately, it also had ZnO phase, which might not resist the flushing of the reactants in the continuous reaction, and its catalytic ability was still relatively low. Thus, it is still a challenging task to develop new heterogeneous catalysts having a good performance for the synthesis of DMC from MC and methanol.

Hydrotalcite (HT) or hydrotalcite-like compounds (HTLcs) are layered double hydroxides belonging to anionic clay with a general formula [M_(1-x)²⁺M_x³⁺(OH)₂]^{x+}·(Aⁿ⁻)_{x/n}·mH₂O, where M²⁺ and M³⁺ are the divalent and trivalent cations, respectively. Their structure is very similar to that of brucite, in which part of the divalent metal ion (M²⁺ = Mg²⁺) could be isomorphously substituted by Al³⁺ or other trivalent metal cations, resulting in the formation of positive charged layers, which in turn is charge compensated by the anions (Aⁿ⁻) such as CO₃²⁻ or OH⁻ present in the interlayer.³¹ More important, the mixed oxides obtained by the thermal decomposition of these compounds possess homogeneous dispersion of M²⁺ and M³⁺ at an atomic level, high stability against sintering, high surface area and tunable basic properties.³²⁻³⁴ Therefore, HTLcs with different composition are among the most investigated catalyst precursors for the remarkable properties of the final catalysts, which have been used in many reactions such as aldol condensation, Michael addition, transesterification and so on.³⁵⁻³⁸ In our previous work, we have reported that Mg-Al mixed oxide catalysts were effective solid base catalysts for the reaction of urea and phenol.³⁹ Very recently, we have discovered the promotion effect of transition metal on the

basicity and activity of calcined hydrotalcite catalysts for the diethyl carbonate synthesis.⁴⁰ However, the effect of rare earth element doping on the basicity of calcined hydrotalcite and their catalytic performance in the DMC synthesis remain unknown. As our continuous research work, here, we wish to show that La-modified Mg-Al mixed oxides (HTC-La) by calcination of corresponding La-containing hydrotalcite-like (HTI) precursors are efficient solid base catalysts for the DMC synthesis from MC and methanol, and the DMC yield could reach 54.3% under optimal reaction conditions. Besides, their activity could be tailored by simple adjustment of La additive amount. The correlations between the textural, chemical structures, the basic properties of the HTC-La catalysts and their catalytic performances in the MC methanolysis were investigated. At the same time, the catalytic activities and recyclability of catalysts were systematically studied. Finally, we proposed a plausible reaction mechanism that MC and methanol were simultaneously activated on the surface basic sites of HTC-La catalysts based on *in situ* FTIR experiments results.

2. Experimental

2.1 Catalyst preparation

La-containing hydrotalcite-like compounds with various Mg²⁺: Al³⁺: La³⁺ atomic ratios were synthesized using the coprecipitation method followed by hydrothermal treatment.⁴¹ The Mg²⁺: Al³⁺: La³⁺ atomic ratio in the starting solution was kept to 3: 1: x, where x was varied from 0 to 1.0. In a typical procedure, two aqueous solutions, a 100 mL solution of Mg²⁺, Al³⁺, La³⁺ nitrates and a 100 mL mixed solution of NaOH and Na₂CO₃ precipitant, were added dropwise to 100 mL deionized water under vigorous stirring. The addition was performed over 1.0-1.5 h and the pH value was maintained close to 10 by addition of suitable amounts of 2 M NaOH solution. The resulted gel-like slurry was transferred into autoclaves and hydrothermally treated at 80 °C for 24 h. Then, the as-prepared product was collected after being filtered and washed with deionized water until the pH of the filter liquor became 7.0. Finally, the precipitate was dried at 100 °C for 12 h to obtain HTI precursors.

The as-prepared HTLcs were further calcined in air at 500 °C for 7 h at a heating-up rate of 5 °C /min to obtain the final mixed oxides catalysts. The synthesized hydrotalcite-like precursors and corresponding mixed oxides were denoted as HT-NLa before calcination and HTC-NLa after calcination, respectively, where N/10 represented the La³⁺: Al³⁺ atomic ratio in the starting solution. For comparison, La₂O₂CO₃ catalyst was prepared under the same condition using La(NO₃)₃·5H₂O as La source and Na₂CO₃ as precipitant, followed by calcination at 500 °C for 7 h in CO₂ atmosphere.

2.2 Characterization

Thermogravimetric analysis (TGA) was performed on a NETZSCH STA-409 thermal analyzer under nitrogen (50 mL/min) with a heating rate of 10 °C /min from room temperature to

800 °C to study the thermal decomposition behavior of catalyst precursors. Power X-ray diffraction (XRD) patterns of the samples were recorded on a Rigaku Miniflex diffractometer using a Cu target with a Ni filter in a 2θ range of 5–80°. The elemental chemical analysis of samples was performed using the inductively coupled plasma-optical (ICP) emission spectroscopy (Thermo iCAP 6300). Nitrogen adsorption-desorption isotherms were obtained at liquid nitrogen temperature, -196 °C on a Micromeritics ASAP-2020 instrument (Norcross, GA), using static adsorption procedures. The samples were degassed at 200 °C for 5 h prior to the measurement. The BET isotherm and BJH were used to obtain specific surface area and pore volume, respectively. The morphology of the samples was investigated using a Hitachi S4800 scanning electron micrograph (SEM) with an accelerating voltage of 20.00 kV. X-ray photoelectron spectroscopy (XPS) measurements were performed over a Thermo Scientific k-Alpha spectrometer equipped with Al anode (Al $K\alpha$ = 1486.6 eV) operating at 72 W and spot size of 400 μm under ultrahigh vacuum (10^{-7} Pa). The binding energies were calibrated internally for surface charging by adventitious carbon deposit C (1s) with E_b = 284.5 eV.

The basic properties of the catalysts were determined by CO₂ temperature-programmed desorption (CO₂-TPD). Catalysts (0.1 g, 40–60 mesh) were placed in the quartz reactor bed. After 5 h pretreatment in Ar flow at 500 °C, the catalysts were cooled to room temperature. Then, they were saturated with pure CO₂ (30 L/min) using a six-way valve for 3 h and then flushed with Ar (40 L/min) flow to remove all physical adsorbed molecules. Afterward, the CO₂-TPD experiments were started from 30 to 500 °C with a heating rate of 10 °C/min under Ar flow (40 L/min), and the desorbed CO₂ was detected by an AMETEK mass spectrometer. CO₂ peak area was quantitatively calibrated by injecting CO₂ pulses.

The *in situ* Fourier transform infrared spectroscopic (FTIR) experiments were performed in a closed stainless FTIR steel cell for scanning at suitable temperatures, and the spectra were recorded with a Nicolet Magna 550 FTIR spectrometer in the region of 4000–400 cm^{-1} at a resolution of 4 cm^{-1} . In the present work, four types of experiments were performed, namely: (a) MC thermal decomposition: 15 mg of MC was ground and pressed to a self-supporting pellet, and then the disk was put into the closed cell; (b) MC adsorption on the catalyst: the sample was obtained by mixing 14 mg catalyst and 1 mg MC, and then ground and pressed to a self-supporting pellet, and then it was put into the closed cell; (c) methanol adsorption on catalyst: 15 mg catalyst was finely ground and pressed to a self-supporting pellet. After pretreated under vacuum for 3 h, 10 μL of methanol was injected into the closed cell. (d) Co-adsorption of MC and methanol on catalyst: the sample was obtained by mixing 14 mg catalyst and 1 mg MC, and then ground and pressed to a self-supporting pellet. After pretreated under vacuum for 3 h, various amounts of methanol (0, 10, 20, 40, 60, 80, 100 μL) was introduced into the closed cell, and the cell was rapidly heated to 180 °C, respectively. Then, the FTIR spectra of co-adsorption of reactants on catalyst were collected at this

temperature. With respect to the (a), (b) and (c) experiments, the FTIR cell was heated from room temperature to 200 °C, and the spectra were collected once every 2 min in this work.

2.3 Catalytic test

The catalytic activities of the catalysts for the synthesis of DMC from MC and methanol were evaluated in a 100 mL stainless steel autoclave reactor equipped with electric heating, a reflux column and a magnetic stirrer under the assigned conditions. In a typical process, 0.5 g the freshly prepared catalysts, 0.05 mol (3.75 g) MC and 1 mol (32 g) methanol were placed in the reactor. Then, it was rapidly heated to 200 °C and kept for 6 h with magnetic stirring. During the reaction, the temperature error was less than 2 °C. After the reaction, the autoclave was cooled to room temperature, and product mixture in the autoclave was weighed, clarified and determined on a gas chromatography with a PEG-20M capillary column and a flame ionization detector (FID). The column was temperature-programmed from 80 to 180 °C.

3. Results and discussion

3.1 Textural and structural properties of the prepared materials

The XRD patterns of the HTI precursors with $\text{Mg}^{2+}:\text{La}^{3+}:\text{Al}^{3+}$ from 3: 1: 0 to 3: 1: 1 are shown in Fig. 1 (a). Obviously, HT-0La and HT-2La precursors exhibited similar profiles to the pure layered double hydroxide structure with sharp and symmetric peaks for (003), (006), (110) and (113) planes and broad asymmetric peaks for (009), (015), and (018) planes (JCPDS 70-2151).³¹ For HT-5La, HT-8La and HT-10La samples, the peaks of a mixture $\text{La}(\text{OH})_3$ (JCPDS 06-0585) and $\text{La}_2(\text{CO}_3)_2(\text{OH})_2$ (JCPDS 70-1774) were also detected.^{42–44} According to previous reports, La favored the formation of lanthanum carbonate species in the very early stages of the co-precipitation because that it possessed the lowest electronegativity compared to other rare earth elements.^{42,43,45} Meanwhile, the La preferred to locate in the interlayer gallery of HT as separated hydroxide and hydroxyl carbonate phases due to its relatively large ionic radius.⁴² On the other hand, the peaks intensities and sharpness of (003) and (006) planes, which were directly proportional to the crystallinity of material, were observed to decrease on increasing of La content of precursors. This might be ascribed to the following reasons. Firstly, La^{3+} possessed higher ionic radius (0.103 nm) than that of Mg^{2+} (0.072 nm) and Al^{3+} (0.053 nm), resulting in large distortions when it was incorporated into the HTI layers. Moreover, it was suggested that high Al content was favorable for the formation of HTI precursor.⁴⁶ In this study, the $\text{La}^{3+}:\text{Al}^{3+}$ atomic ratios in the starting solution increased from 0:1 to 1:1, so the Al content decreased relatively with increasing of La content. Consequently, the yields of the HTI phase in the precursors decreased and such HTI structure almost disappeared when x reached 1.0.

It was well known that HTICs belonged to the hexagonal crystal system, and they could be described by two important values, a and c .³¹ As seen in Table 1, both the parameters a

and c of La-containing HTI precursors increased with the increase of La content, and values of these parameters were in good agreement with those reported by others.^{42,43} The parameter a ($a = 2d_{110}$) was a function of average radius of the metal cations in the layers and reflected the density of metal ions in the (110) plane. The increase of a parameter might be owing to the isomorphous substitution of Mg^{2+} or Al^{3+} by La^{3+} in the HTI layers. La^{3+} exhibited larger ionic radius in comparison with Mg^{2+} and Al^{3+} , thus more La^{3+} insertion into brucite sheets led to an increase of average radius of the cations in the layers.⁴⁴ The parameter c ($c = 3d_{003}$) was a measure of the thickness of the HTI layer and the interlayer distance, which was further relied on the electrostatic force in the HTI interlayer. Due to its larger ionic radius, La^{3+} exhibited lower charge density than that of Mg^{2+} and Al^{3+} . Thus, the insertion of La^{3+} into HTI layer would cause a decrease of electrostatic forces between the layer and interlayer. In addition, La^{3+} preferred to locate in the interlayer gallery of HT as separate hydroxyl carbonate phases, which resulted in the decrease of the electrostatic attraction between the layers and interlayers anions, leading to the increase of the layer spacing.⁴²

The XRD patterns of the samples after calcination are shown in Fig. 1 (b). Clearly, heat treatment of the HTICs at 500 °C destroyed the HTI structure since no characteristic reflections peaks of HTICs were found in the XRD patterns. All of these calcined materials presented reflections at 43.3° and 62.8° owing to (200) and (220) planes, respectively, of MgO-periclase (JCPDS 45-0946) phase. Nevertheless, the intensity of peaks due to MgO-periclase were decreased and almost vanished when the La additive amount reached $x = 1.0$. Diffraction peaks assigned to Al_2O_3 were not found in the calcined catalysts, implying that Al_2O_3 might exist in an amorphous state. As the x increased to 0.5, the diffraction peaks ascribed to monoclinic $La_2O_2CO_3$ (JCPDS 48-1113) formed by re-adsorption of gaseous CO_2 , coming from the HTICs decomposition or air contamination during the sample manipulation were detected.⁴²⁻⁴⁴ As to HTC-8La and HTC-10La materials, the diffraction peaks of hexagonal $La_2O_2CO_3$ (JCPDS 37-804) also appeared at 2θ of 11.0°, 22.2°, 25.2°, 27.6°, 30.5°, 33.6°, 44.4°, 47.4° and 50.3°, which indicated that higher content of La was favorable for the $La_2O_2CO_3$ crystal transformation from monoclinic to hexagonal. In addition, the formation of $La_2O_2CO_3$ led to the peaks of the (200) phase of MgO shift to lower angles, which probably because that some La^{3+} ions had incorporated into MgO lattice.

Fig. 2 shows the weight loss and the weight loss rates of the HTICs during calcination, which reveals the transformation of HTI samples into the corresponding mixed oxides. Obviously, the TG profile of pure Mg-Al hydrotalcite (HT-0La) precursor consisted of two major steps, while the La-containing HTICs showed four typical weight losses. The first loss for all the samples was associated with a peak at 175-218 °C with a shoulder peak at 67-85 °C. According to previous literatures, it was owing to the removal of physical absorbed water, interlayer water molecules and small amounts of weakly bound OH groups. The second weight loss at 360-410 °C is due

to the elimination of both the hydroxyl groups from HTI network and carbonate anions from the interlayer anion, resulting in the collapse of the layered structure.⁴⁷ With regard to La-containing precursors, the third weight loss at 420-440 °C might be ascribed to dehydroxylation of La-OH, resulting in transformation La hydroxide and hydroxyl carbonate phases into $La_2O_2CO_3$.⁴⁸ Furthermore, another weight loss was also found at around 710 °C in La-containing HTICs, which might be because of the thermal decomposition of $La_2O_2CO_3$.⁴⁹ Obviously, this weight loss became more and more intense with increasing of La content. This phenomenon was consistent with the result of XRD, which showed that the number of $La_2O_2CO_3$ peaks increased from HTC-2La to HTC-10La samples.

The weight losses for the second and third steps are compared in Table 1. It could be seen that with increasing of La content, the second weight loss step due to decomposition of the HTI species, decreased, while the third weight loss, owing to La hydroxide and hydroxyl carbonate phases, increased. This suggested that the higher the $La^{3+}:Al^{3+}$ atomic ratio in the mother liquid, the less HTI phases and the more separated La hydroxide and hydroxyl carbonate phases existed in the precursors, which was in accordance with the XRD patterns of these samples. In addition, the TG profiles demonstrated that the introduction of La led to a decreasing of the decomposition temperatures, especially for the third weight loss in La-containing HTICs (for example, HT-2La: 440 °C; HT-5La: 435 °C; HT-8La: 429 °C; HT-10La: 420 °C). Furthermore, compared with HT-0La sample, the second step position in La-containing precursors also shifted toward lower temperature with the increasing of La content. These results implied a gradual decrease of the thermal stability of the La-containing HTICs when x increased from 0.2 to 1.0. It might be ascribed to the presence of separated lanthanum hydroxide and hydroxyl carbonate phase in the interlayer space, which led to a decrease of the electrostatic attraction between the layers and the interlayer anions that resulted in the increase of the interlayer space and lower thermal stability.^{42,49}

In the present work, surface compositions of the calcined samples, as determined by XPS are compared with the chemical compositions of the catalysts measured by ICP in Table 2. It was clearly observed that the surface was considerably depleted of La, while the same surface was enriched in Mg and Al for La-modified Mg-Al mixed oxides. This was in accordance with the results in previous report, where La: Zn atomic ratios in surface were decreased significantly when Zn-Al-La HTICs were prepared.⁴⁹

The textural properties of HTC-La catalysts were valued by N_2 adsorption-desorption technique. The N_2 adsorption-desorption isotherms and the corresponding pore sized distribution of calcined samples are shown in Fig. 3. Apparently, all the samples showed typical type-IV adsorption isotherms with clear hysteresis loops at higher relative pressure, characteristic of a mesoporous solid, and their pore sized were widely distributed at range of 5-45 nm. These hysteresis loops were narrow, indicating that the mesoporous pores were regular. Besides, the hysteresis loops exhibited feature of H3 type (IUPAC classification). It was well

known that this type hysteresis was usually related to materials consisting of platy shaped particles. This was consistent with the traditional view of these types of mixed oxides derived from HTICs.⁵⁰ The specific surface area and pore volume of the calcined samples are listed in Table 2. It could be found that the calcined samples had higher surface area and pore volume than that of corresponding HTIs (see Table 1), which could be ascribed to that a large amount of CO₂ was released from HTICs during calcination.⁴¹ This might be favorable for them to exhibit high catalytic ability. Prescott *et al.* and Meher *et al.* have reported that a high content of Al₂O₃ in the catalysts was favorable to increase the specific area.^{51,52} Besides, as discovered by Cantrell *et al.*, Al favored higher CO₃²⁻ contents in the interlayer, therefore more open porous networks were formed after thermal treatment.⁵³ In this work, as the increasing of La content, correspondingly, the content of Al decreased relatively in these La-containing mixed oxides. At the same time, La might incorporate into pore system of HTC-La catalysts during the preparation process. So, their surface area and pore volume became lower as x increased from 0 to 1.0 (see Table 2). Furthermore, the lowest surface area of HTC-10La, which was not favorable for the exposure of more active sites, could also be owing to the formation of large sintered particles (see SEM profiles).⁴⁹

The morphologies of the HTI precursors are shown in Fig. 4. All the HTI samples consisted mainly of well-developed and plate-shaped crystals, which suggested the formation of a layered structure. For pure Mg-Al HT (HT-0La) material, it exhibited mainly hexagonal plate-shaped crystals, which was the same as the result in previous literature.³⁸ However, the plate-crystals surface became rough and indistinct with the increasing of La additive amount. This also implied that the introduction of lanthanum was not favorable for the synthesis of HTI structure, which was in agreement with the XRD results and previous reports.^{42,43,49} The particles of the samples calcined after 500 °C maintained the similar morphology of the precursors, though some crystals were destroyed (see Fig. 5). Meanwhile, their particles seemed to be sintered and the particle size of the calcined samples increased as the La additive amount increased. This might be because of the formation La₂O₂CO₃ phase in the catalysts, which was proved by the XRD patterns in Fig. 1 (b). Considering their surface area decreased with the increasing of La additive amount, it was reasonable to suggest that less La₂O₂CO₃ phase and smaller particle size favor the formation of mixed oxide catalysts with higher specific surface.

3.2 The surface basicity of catalysts

For solid base catalysts, two factors including basic strength and total basicity (basic sites amount per unit weight of catalysts) were selected to evaluate their surface basic property.⁵⁴ Here, the surface basic property of catalysts was examined by CO₂-TPD and the basic species could be assigned according to the temperature at which peaks appeared. Higher desorption temperature pointed to stronger basic strength and more CO₂ uptake indicated higher total basicity. Fig. 6

shows the CO₂ desorption profiles for the prepared La-modified Mg-Al mixed oxides. For comparison, the produced La₂O₂CO₃ sample was also investigated. Apparently, the TPD profiles of these samples could be split into three Gaussian peaks, indicating that three types of basic sites with different strengths were present on each surface. Depending on the temperature of desorption, these desorption peaks could be assigned to weak (CO₂ desorption below 200 °C), moderate (CO₂ desorption between 200 and 400 °C) and strong (CO₂ desorption higher than 400 °C) basic sites. According to the description of reported studies, the weak basic sites were related to OH⁻ groups, moderate basic sites were associated with metal-oxygen pairs (such as Mg-O, Al-O, and La-O), and strong basic sites were assigned to low-coordination unsaturated oxygen atoms, respectively.^{38,41,55} And from the CO₂-TPD profiles of HTC-La samples, both the moderate and strong basic sites gradually shifted to higher temperature with the rise of La content, which suggested that a greater amounts of La content resulted in the increase of moderate and strong basic strength. Moreover, it should be mentioned that among all the samples, La₂O₂CO₃ showed the highest desorption temperature of the strong basic site at about 437 °C. Thus, based on CO₂-TPD characterization, the basic strength of these catalysts followed this order: La₂O₂CO₃ > HTC-10La > HTC-8La > HTC-5La > HTC-2La > HTC-0La.

On the other hand, the basicity of all the samples is listed in Table 2. One can see that La₂O₂CO₃ catalyst showed the least total basicity, which might be due to its low specific surface area resulting in decreasing its exposed basic sites. Moreover, the contribution of the weak basic site to total basic sites was about 50%. For the La-containing mixed oxides, this proportion decreased with increasing of La additive amount, and their moderate and strong basic peaks was more intense (72.9%-89.6% of total number of basic sites). Therefore, the presence of La not only improved the basic strength, but also promoted the amounts of moderate and strong basic sites of HTC-La catalysts. Notably, although the number of strong basic sites of HTC-La increased as the increasing of La content, the amount of moderate basic sites increased first, and reached the maximum when x was 0.5. Then, it gradually decreased with further increasing of La content. These results revealed that except for BET surface area, there was some other cause that was responsible for the change of the number of moderate and strong basic sites. In theory, introduction of La could increase the amount of metal-oxygen pairs (La-O) on the catalyst surface, and led to the rise of the number of moderate basic sites for metal oxides. Nevertheless, as reported by Wu *et al.*, the metal-oxygen could partially break up, which led to the generation of coordinatively unsaturated O²⁻ ions, and the lower stability of layered structure was beneficial to the formation of unsaturated O²⁻ ions.⁵⁶ According to the above analysis based on TGA, a gradual decrease of the thermal stability of the La-containing HTICs was found when x increased from 0 to 1.0. Consequently, metal-oxygen in the mixed oxides would gradually transform to unsaturated O²⁻ ions as the increasing of La content. Therefore, it seemed that both BET surface areas and La content could affect the number of basic

sites and surface basic site distribution for HTC-La catalysts. Considering the amounts of both moderate and strong basic sites, their basic densities decreased in the following sequence: HTC-5La (212.7 $\mu\text{mol/g}$) > HTC-8La (200.4 $\mu\text{mol/g}$) > HTC-10La (189.6 $\mu\text{mol/g}$) > HTC-2La (163.2 $\mu\text{mol/g}$) > HTC-0La (125.4 $\mu\text{mol/g}$) > $\text{La}_2\text{O}_2\text{CO}_3$ (55.1 $\mu\text{mol/g}$). So, for HTC-La catalysts, their basicity of moderate and strong basic sites first increased until $x = 0.5$, then decreased with further increased of La content.

3.3 Catalytic performance

3.3.1 The reaction system of MC and methanol to synthesize DMC

It was well known that the reaction system of MC and methanol could be described by expressions 1-3 in Scheme 1 no matter what catalysts were used.

At first, DMC could be synthesized via the substitution of the amino group of MC by the methoxy group in methanol. The product DMC, which was a favorable methylating agent for amino group, could further react with MC to yield *N*-methyl methyl carbamate (NMMC).¹² Furthermore, at a relatively high reaction temperature, DMC was easily thermal decomposed into dimethyl ether (DME) and carbon dioxide in the present of solid basic and acidic oxides.^{57,58} It should be mentioned that DME could not be detected by GC because it was easy to volatilize when the autoclave was opened.¹⁸⁻²⁴ Thus, the catalysts were evaluated on the basis of MC conversion, DMC yield and selectivity, and NMMC yield in the present case.

3.3.2 Effect of La content on the DMC synthesis

The catalytic performances of various catalysts were evaluated for the methanolysis of MC to DMC. The results are summarized in Table 3. Notably, the reaction of MC and methanol hardly occurred in the absence of catalyst (entry 1). However, HTC-0La exhibited high activity towards the DMC synthesis, yielding 28.2% DMC. The catalytic performances of La-containing mixed oxide catalysts are presented in entries 3-6. The four catalysts all gave higher MC conversion compared to HTC-0La sample, indicating they had higher catalytic activities. Nevertheless, the DMC yield and selectivity differed significantly among them. When HTC-2La catalyst was used, 34.7% yield of DMC was achieved, which was a bit higher than that of HTC-0La. Under the same reaction condition, HTC-5La possessed an excellent catalytic performance with a high DMC yield of 54.3% and a good DMC selectivity of 80.9%. As the La additive amounts further increasing, both the MC conversion and the DMC selectivity decreased remarkably. For instance, HTC-8La and HTC-10La catalysts gave 43.2% and 33.8% DMC yield, respectively. At the same time, their selectivity decreased to 72.6% and 64.5%, respectively. Besides, a further investigation on the performance of prepared $\text{La}_2\text{O}_2\text{CO}_3$ was also conducted. Obviously, it showed inferior activity than the aforementioned mixed oxide catalysts (entry 7). More important, it was noteworthy that for these catalysts, their catalytic activities decreased in sequence of HTC-5La > HTC-8La > HTC-10La > HTC-2La > HTC-0La > $\text{La}_2\text{O}_2\text{CO}_3$. While, the DMC selectivity achieved over them followed this order: HTC-

0La > HTC-2La > HTC-5La > HTC-8La > HTC-10La > $\text{La}_2\text{O}_2\text{CO}_3$. So, the current catalytic performance tests suggested that the insertion of La into Mg-Al mixed oxides could remarkably improve the DMC synthesis from MC and methanol.

3.3.3 Effect of basic property on the DMC synthesis

For catalyst, increase in their BET surface areas was favorable for achieving higher catalytic ability. The surface areas of the catalysts are listed in Table 2. It could be seen that their BET surface areas decreased in the order of HTC-0La > HTC-2La > HTC-5La > HTC-8La > HTC-10La > $\text{La}_2\text{O}_2\text{CO}_3$. However, their catalytic activity followed this sequence: HTC-5La > HTC-8La > HTC-10La > HTC-2La > HTC-0La > $\text{La}_2\text{O}_2\text{CO}_3$. Thus, the BET surface area of catalysts was not the sole factor for their catalytic ability in the present work. As the discussion above-mentioned, the moderate and strong basic sites of HTC-La samples were enhanced remarkably; therefore, their catalytic activities might be closely related to the amounts of moderate and strong basic sites. In addition, it should be noted that the DMC selectivity decreased as the increase of basic strength of strong basic sites. In order to well clarify the correlation between the MC conversion and the amounts of both moderate and strong basic sites, as well as the relationship between their DMC selectivity and basic strength, we illustrated the catalytic performance at 2 h when the reaction was at the beginning in Fig. 7. It could be found that the sequence of MC conversion was in good agreement with the trend of basicity of both of moderate and strong basic sites (Fig.7 (a)); whereas a contrary trend for DMC selectivity was observed to the order of their basic strength (Fig.7 (b)). These phenomena further suggested that the amounts of moderate and strong basic sites played a crucial role for MC conversion. However, a too strong basic strength was not beneficial to obtaining high DMC selectivity, which might be because that the side reactions such as thermal decomposition of DMC and NMMC synthesis would aggravate over strong basic catalysts.^{57,58} This was consistent with the results in previous work, in which the DMC selectivity also decreased with rise of basic strength when basic oxide such as CaO, La_2O_3 and MgO were used as the catalysts.¹² Therefore, it was reasonable to draw the conclusion that the enhancement of catalytic performance for La-modified Mg-Al mixed oxide catalysts towards DMC synthesis from MC and methanol was owing to the adjustment of the basic property by incorporation of suitable amount of La additive.

3.3.4 Effect of reaction conditions over HTC-5La catalyst

The reaction conditions were further optimized over HTC-5La catalyst. The effect of reaction temperature on the DMC synthesis is illustrated in Fig. 8 (a). Obviously, the reaction temperature exhibited a significant impact on the reaction. The conversion of MC consistently enhanced with the increase of temperature. However, the DMC yield and selectivity increased sharply in the temperature range of 180-200 °C, and then decreased when the reaction temperature exceeded 200 °C. It could be seen that the maximum DMC yield of 54.3% with the highest DMC selectivity of 80.9% was obtained when

the reaction temperature was 200 °C. Theoretically, the DMC synthesis was endothermic reaction and the temperature had a positive effect on DMC formation.¹⁹ However, higher temperature also shortened the time needed to reach maximum DMC concentration and accelerated the rate of side reactions including *N*-methylation of MC. As a result, the yield of by-product NMMC increased significantly to 6.4% at the cost of DMC consumption when the reaction temperature was 210 °C. Therefore, the suitable reaction temperature should be 200 °C.

The effect of reaction time on the DMC synthesis is demonstrated in Fig. 8 (b). Clearly, as the reaction proceeded, the conversion of MC increased. DMC yield and selectivity reached their maximal values at 6 h, and then, the consumption of DMC in the further reaction surpassed gradually the formation of DMC from MC. Thus, the suitable reaction time was chosen as 6 h.

The effect of catalyst amount was also studied and the results are shown in Fig. 8 (c). With the increase of catalyst amount, the conversion of MC always monotonically increased, but the DMC yield and selectivity reached the maximum values of 54.3% and 80.9% at 0.5 g and then decreased. It was ascribed to that the yield of further reaction product NMMC increased gradually if catalyst amount was more than 0.5 g. Therefore, the suitable catalyst amount was chosen as 0.5 g in the present case.

The effect of methanol/MC molar ratio on DMC synthesis is presented in Fig. 8(d). The results demonstrate clearly that the DMC yield and selectivity increased first in the range of 10–20 and then decreased in the range of 20–25. When the methanol/MC molar ratio was 20, the DMC yield and selectivity reached the maximum 54.3% and 80.9%, respectively. When the methanol/MC molar ratio was lower than 20, MC concentration was higher and the side-reaction of *N*-methylation of MC with DMC would occur easily, resulting in lower DMC yield and selectivity. In theory, a higher methanol/MC molar ratio could promote the reaction equilibrium towards the DMC synthesis. Nevertheless, a too high methanol/MC molar ratio would lead to the reduction of MC concentration. Besides, the following *in situ* FTIR experiments revealed that MC and methanol molecules were co-absorbed on the surface basic sites of HTC-5La catalyst. Consequently, some active sites of catalyst for activating MC would be occupied by a larger amount of methanol. Thus, the reaction rate might decrease resulting in a lower DMC yield when methanol/MC molar ratio exceeded 20. In the present case, from the practical view, the suitable methanol/MC molar ratio was selected as 20.

3.3.5 Reusability and stability of HTC-5La catalyst

Reusability of catalysts played a crucial role for the DMC synthesis via MC methanolysis in practical industrial production. Therefore, in order to explore a highly effective and stable solid catalyst, the reusability of HTC-5La was also investigated. After the first run, used HTC-5La sample was separated by filtrating, and washed with methanol several times, dried in oven at 80 °C and reused without any pre-

treatment. Their catalytic performance was evaluated and the results are shown in Fig. 9. To our delight, HTC-5La could be recycled and reused at least four times without obvious loss of activity. At the same time, the recovered HTC-5La catalyst after reused four times (HTC-5La-fourth) was analyzed using SEM and XRD techniques. SEM presented that the plate-like morphology was unchanged after the catalyst was used four times (see Fig. 5). Additionally, the XRD pattern of HTC-5La-fourth is shown in Fig. 1(b). Obviously, its diffraction peak number was as the same as the fresh one, and the peak intensity didn't show any significant change. Therefore, the HTC-5La catalyst possessed higher stability than previously reported zinc-based catalysts for this reaction and a heterogeneous solid catalyst with excellent catalytic performance and stability was successfully developed.

3.4 FTIR spectra between reactants and HTC-5La catalyst

The adsorption behaviours on the solid catalyst surface play an important role for the reaction pathways. In order to investigate the possible mechanism of the reaction between MC and methanol, *in situ* FTIR experiments under different conditions were conducted.

3.4.1 MC decomposition

Fig. 10 (a) demonstrates the FTIR spectra evolution of MC with increasing of temperature. At room temperature, the characteristic bands of MC that ascribed to the C=O stretching vibration (amide I band) and NH₂ bending vibration (amide II band) were observed at 1700 and 1610 cm⁻¹, respectively.⁵⁹ It was worth noting that a new band appeared at 2198 cm⁻¹, which was assigned to N=C=O asymmetric stretching vibration of isocyanic acid when the temperature surpassed 140 °C.^{17,60} Apparently, the intensity of the bands attributed to MC decreased, accompanying that of the band at 2198 cm⁻¹ increased rapidly with further increase of temperature. This implied that the formation of isocyanic acid was due to the decomposition of MC, which was in accordance with the results discovered by Li *et al.*⁶⁰

3.4.2 MC adsorption on HTC-5La catalyst

Then, the adsorption of MC over HTC-5La catalyst was studied at given temperature regions, and the FTIR spectra are shown in Fig. 10 (b). Clearly, the intensity of both amide I and amide II bands of MC decreased rapidly as the temperature increased. At the same time, the amide I band showed a blue shift gradually from 1700 to 1728 cm⁻¹, accompanying the red shift of the amide II band from 1610 to 1598 cm⁻¹ before they disappeared, which did not occur when pure MC decomposed. These alternations pointed out the interaction of nitrogen in MC with unsaturated metal cations site on HTC-5La catalyst, resulting in the amino group of MC bound to metal oxide surface (M-NH₂).⁶¹ More important, a new band assigned to stretching vibration of N=C=O bound to metal oxide surface (M-N=C=O, M= Mg, Al or La) was found at around 2190 cm⁻¹. It could be seen that the intensity of N=C=O increased first before the temperature increase to 160 °C, implying that MC

was swiftly activated and decomposed into isocyanic acid over the catalyst. However, its intensity decreased with further increase of temperature, suggesting the enhanced desorption of isocyanate-containing species. In addition, compared to the blank test without the catalyst, the characteristic band of $\text{N}=\text{C}=\text{O}$ was clearly observed at a lower temperature of $80\text{ }^{\circ}\text{C}$ on HTC-5La catalyst surface. Thus, all these results proved that MC could be activated over HTC-5La catalyst and the characteristic band of $\text{N}=\text{C}=\text{O}$ still existed when the temperature increased to $200\text{ }^{\circ}\text{C}$.

3.4.3 Methanol adsorption on HTC-5La catalyst

Fig. 10 (c) illustrates the FTIR spectra evolution of methanol adsorbed on HTC-5La catalyst at different temperatures. Two new bands at 2395 and 2823 cm^{-1} corresponding to C-H asymmetric and symmetrical stretching vibrations of deprotonated methanol, or methoxide species were clearly visible, which indicated the adsorption of methoxyl group on the surface of HTC-5La catalyst. This was in accordance with previously reported studies of adsorbed methanol on metal oxide catalysts.^{22,62} Thus, these experimental results suggested that methanol could be activated and deprotonated over HTC-5La catalyst, resulting in formation of methoxide species coordinated to metal atoms. Moreover, the two bands became more and more obvious at higher temperature, implying that methanol was prone to methoxy groups on the catalyst surface at higher temperature.

3.4.4 Co-adsorption of MC and methanol on HTC-5La catalyst

In order to study the reaction procedure on HTC-5La catalyst more clearly, we carried out the MC and methanol co-adsorption experiments (see Fig. 10 (d)). In the present case, we followed the change of the band at 2190 cm^{-1} corresponding to stretching vibration of $\text{N}=\text{C}=\text{O}$ bound to metal oxide surface ($\text{M}-\text{N}=\text{C}=\text{O}$), the band at 1750 cm^{-1} assigned to $\text{C}=\text{O}$ stretching vibration of DMC,⁶³ as well as the amide I and II bands of MC. Without methanol, MC was activated and decomposed into isocyanic acid species by the basic sites of catalyst. As the amount of methanol increased, the intensity of $\text{M}-\text{N}=\text{C}=\text{O}$ decreased quickly and disappeared when the amount of methanol increased to $40\text{ }\mu\text{L}$. During this process, the characteristic bands of MC were found at about 1700 and 1610 cm^{-1} . This revealed the decomposition of MC might be a reversible reaction, and MC would be re-generated via the reaction between methanol and isocyanic acid species when excessive methanol existed in reaction system. At the same time, it should be noted that for MC molecule, its amide I band had a blue shift, while the amide II band showed a red shift before they disappeared. This also implied that MC was adsorbed on the catalyst surface and its amino group was coordinated with the cationic metal surface atom ($\text{M}-\text{NH}_2$).⁶¹ Besides, a new band at 1750 cm^{-1} ascribed to DMC was detected when the methanol amount was $60\text{ }\mu\text{L}$. Apparently, the amide I and II bands of MC decreased rapidly with the further increasing of methanol amount and they vanished as the amount of methanol reached $100\text{ }\mu\text{L}$. Meanwhile, the

intensity of characteristic band of DMC consistently enhanced during this process, revealing the production of DMC from MC and methanol over the HTC-5La catalyst.

3.4.5 Plausible reaction mechanism for DMC synthesis from MC and methanol

According to the FTIR experimental results and previous work,⁶⁰ a plausible basic catalytic mechanism that MC and methanol were activated simultaneously on the surface basic sites of HTC-5La catalyst was proposed. As shown in Scheme 2, MC was adsorbed on catalyst surface through its amino group bound to metal oxide surface. Consequently, MC was easily decomposed into isocyanic acid. As the discussion above-mentioned, the decomposition of MC into isocyanic acid and methanol might be a reversible reaction. In this work, because the molar ratio of methanol/MC was selected as 20, the reaction equilibrium would shift to MC formation in presence of excessive methanol in a short time. Then, the re-synthesized MC was coordinated with the cationic surface metal (Mg, Al or La) atom of mixed oxide through the N atom of amino group. As a result, the electrons of C-N group of MC would be redistributed and then, the proton moved to the carbon atom with the appearance of carbocation and nitrogen anion. At the same time, the HTC-5La catalyst could also activate methanol through the abstraction of $\text{H}^{\delta+}$ by the basic sites, giving a strong nucleophilic methoxy group, which formed a complex with the unsaturated metal cations of the catalyst. Subsequently, a lone pair of electrons of the oxygen atom in the methoxy group formed a bond with the electrophilic carbonyl carbon of activated MC to generate DMC, while the hydrogen proton breaking away from the methanol molecule combined with the amino group leaving from the activated MC molecule to form NH_3 .

3.5 Activity comparison of HTC-5La catalyst with other reference catalysts

In this work, the catalytic activity of HTC-5La catalyst is compared with several representative catalysts and the comparative results are listed in Table S1 in ESI. Homogeneous catalysts such as ZnCl_2 and LaCl_3 possessed good catalytic performance,^{28,29} but they were inconvenient for catalyst recovery in practical production. Although ZnO exhibited high catalytic ability towards the reaction between urea and methanol,¹⁹ it was almost inactive for this reaction.²⁴ In fact, it was a precursor of homogeneous catalyst for the reaction of urea and methanol.²⁴ Compared to pure oxide CaO ,¹² Fe_2O_3 supported on MCM-49 ($\text{Fe}_2\text{O}_3/\text{HMCM-49}$) showed higher catalytic activity with 97.3% DMC selectivity.¹⁸ Unfortunately, the DMC yield was lower than 35%. Besides, Zn/Al ,²² Zn/Fe ,³⁰ and $\text{ZnO}-\text{CeO}_2-\text{La}_2\text{O}_3$ mixed oxides²³ were often used to catalyze the DMC synthesis. Even though these catalysts were highly active, their reusability might be limited. The present HTC-5La catalyst showed higher activity compared to the other reported solid catalysts. In addition, the present catalyst was reusable, and its preparation method was simple and repeatable. Based on above results, we can conclude that the

HTC-5La sample is an active, stable and practical catalyst for the DMC synthesis from MC and methanol.

4. Conclusions

The La-modified mesoporous Mg-Al mixed oxides derived from hydrotalcite-like compounds containing La ($Mg^{2+}:Al^{3+}=3$) with $La^{3+}:Al^{3+}$ from 0 to 1.0 were synthesized via a simple co-precipitation method followed by hydrothermal treatment. The La content had a significant influence on the physicochemical and catalytic properties of the HTC-La catalysts for the synthesis of DMC from MC and methanol. The following conclusions might be drawn:

(1) The pure and crystalline Mg-Al-La hydrotalcite-like compounds could be obtained by addition suitable amounts of La into pure Mg-Al hydrotalcite, and the yields of hydrotalcite-like decreased with increasing of La content.

(2) La could be used to fine-tune the structural, textural and chemical properties of the pure Mg-Al mixed oxide. With the increased $La^{3+}:Al^{3+}$ atomic ratio, the basic strength of HTC-La monotonically enhanced. However, the basicity of moderate and strong basic sites first increased until $La^{3+}:Al^{3+}=0.5$, then decreased with further increased of La content.

(3) Both the basic strength and basicity of HTC-La catalysts were demonstrated to have significant impact on the DMC synthesis. It was found that the catalysts that possessed more moderate and strong basic sites could give high MC conversion. On contrast, DMC selectivity decreased as the increased of basic strength. A suitable amount of La was favorable for the DMC synthesis, and an excellent DMC yield of 54.3% with a high DMC selectivity of 80.9% could be achieved over HTC-5La catalyst. Simultaneously, this catalyst exhibited high stability on the basis of reusability test and SEM, XRD and N_2 adsorption-desorption characterization.

(4) The *in situ* FTIR experiments revealed that MC and methanol were co-adsorption on the surface of HTC-5La sample. Further study indicated that MC was decomposed into metal isocyanato group, and methanol was activated to produce a strong nucleophilic methoxyl group by the basic sites. Finally, a plausible basic catalytic mechanism was proposed for this catalytic reaction.

Acknowledgements

This work is financially supported by the "Strategic Priority Research Program-Climate Change: Carbon Budget and Related Issues" of the Chinese Academy of Sciences Grants (XDA05010108), National Natural Science Foundation of China (21401164), the Natural Science Foundation of Shandong Province, China (ZR2012BL07, ZR2013BL019), and State Key Laboratory of Coal Conversion Open Foundation (J12-13-609).

Notes and references

- 1 Y. Ono, *Appl. Catal. A: Gen.*, 1997, **155**, 133-166.
- 2 A. Dibenedetto and A. Angelini, *Adv. Inorg. Chem.*, 2014, **66**, 25-81.

- 3 P. Rounce, A. Tsolakis, P. Leung and A. York, *Energy Fuels*, 2010, **24**, 4812-4819.
- 4 S. Megahed and W. Ebner, *J. Power Sources*, 1995, **54**, 155-162.
- 5 H. Hood and H. R. Mordock, *J. Phys. Chem.*, 1919, **23**, 498-512.
- 6 Sh. Wang, L. Wei, Y. Dong, Y. Zhao and X. Ma, *Catal. Commun.*, 2015, **72**, 43-48.
- 7 P. Kumar, V. C. Srivastava and I. M. Mishra, *Catal. Commun.*, 2015, **60**, 27-31.
- 8 B. A. Santos, V. M. Silva, J. M. Loureiro and A. E. Rodrigues, *ChemBioEng Rev.*, 2014, **1**, 214-229.
- 9 M. Zhang, M. Xiao, Sh. Wang, D. Han, Y. Lu and Y. Meng, *J. Clean. Prod.*, 2015, **103**, 847-853.
- 10 D. C. Stoian, E. Taboada, J. Llorca, E. Molins, F. Medina and A. M. Segarra, *Chem. Commun.*, 2013, **49**, 5489-5491.
- 11 P. Ball, H. Fuellmann and W. Heitz, *Angew. Chem., Int. Ed. Engl.*, 1980, **19**, 718-720.
- 12 M. H. Wang, H. Wang, N. Zhao, W. Wei and Y. H. Sun, *Catal. Commun.*, 2006, **7**, 6-10.
- 13 J. J. Sun, B. L. Yang and H. Y. Lin, *Chem. Eng. Technol.*, 2004, **27**, 435-439.
- 14 T. Cho, T. Tamura, T. Cho and K. Suzuki, *US Pat.*, 5534649, 1996.
- 15 B. L. Yang, D. P. Wang, H. Y. Lin, J. J. Sun and X. P. Wang, *Catal. Commun.*, 2006, **7**, 472-477.
- 16 H. Wang, B. Lu, X. G. Wang, J. W. Zhang and Q. H. Cai, *Fuel Process. Technol.*, 2009, **90**, 1198-1201.
- 17 Q. B. Li, N. Zhao, W. Wei and Y. H. Sun, *J. Mol. Catal. A: Chem.*, 2007, **270**, 44-49.
- 18 Ch. Zhang, B. Lu, X. G. Wang, J. X. Zhao and Q. H. Cai, *Catal. Sci. Technol.*, 2012, **2**, 305-309.
- 19 M. H. Wang, N. Zhao, W. Wei and Y. H. Sun, *Ind. Eng. Chem. Res.*, 2005, **44**, 7596-7599.
- 20 W. Joe, H. J. Lee, U. G. Hong, Y. S. Ahn, C. J. Song, R. J. Lwon and I. K. Song, *J. Ind. Eng. Chem.*, 2012, **18**, 1018-1022.
- 21 X. M. Wu, M. Kang, N. Zhao, W. Wei and Y. H. Sun, *Catal. Commun.*, 2014, **46**, 46-50.
- 22 X. M. Wu, M. Kang, Y. L. Yin, F. Wang, N. Zhao, F. K. Xiao, W. Wei and Y. H. Sun, *Appl. Catal. A: Gen.*, 2014, **473**, 13-20.
- 23 W. Joe, H. J. Lee, U. G. Hong, Y. S. Ahn, C. J. Song, R. J. Lwon and I. K. Song, *J. Ind. Eng. Chem.*, 2012, **18**, 1730-1735.
- 24 W. B. Zhao, W. C. Peng, D. F. Wang, N. Zhao, J. P. Li, F. K. Xiao, W. Wei and Y. H. Sun, *Catal. Commun.*, 2009, **10**, 655-658.
- 25 H. An, X. Zhao, L. Guo, C. Jia, B. Yuan and Y. Wang, *Appl. Catal. A: Gen.*, 2012, **433-434**, 229-235.
- 26 S. Fujita, Y. Yamanishi and M. Arai, *J. Catal.*, 2013, **297**, 137-141.
- 27 W. B. Zhao, X. Y. Qin, Y. H. Li, Z. S. Zhang and W. Wei, *Ind. Eng. Chem. Res.*, 2012, **51**, 16580-16589.
- 28 W. B. Zhao, F. Wang, W. C. Peng, N. Zhao, J. P. Li, F. K. Xiao, W. Wei and Y. H. Sun, *Ind. Eng. Chem. Res.*, 2008, **47**, 5913-5917.
- 29 D. F. Wang, X. L. Zhang, Y. Y. Gao, F. K. Xiao, W. Wei and Y. H. Sun, *Fuel Process. Technol.*, 2010, **91**, 1081-1086.
- 30 D. F. Wang, X. L. Zhang, Y. Y. Gao, F. K. Xiao, W. Wei and Y. H. Sun, *Catal. Commun.*, 2010, **11**, 430-433.
- 31 F. Cavani, F. Trifirò and A. Vaccari, *Catal. Today*, 1991, **11**, 173-301.
- 32 L. H. Zhang, C. Zheng, F. Li, D. G. Evans and X. Duan, *J. Mater. Sci.*, 2008, **43**, 237-243.
- 33 P. Gao, F. Li, H. J. Zhan, N. Zhao, F. K. Xiao, W. Wei, L. S. Zhong, H. Wang and Y. H. Sun, *J. Catal.*, 2013, **298**, 51-60.
- 34 G. Busca, U. Costantino, F. Marmottini, T. Montanari, P. Patrono, F. Pinzari and G. Ramis, *Appl. Catal. A: Gen.*, 2006, **310**, 70-78.

- 35 L. Faba, E. Díaz and S. Ordóñez, *Appl. Catal. B: Environ.*, 2012, **113-114**, 201-211.
- 36 D. Tichit, D. Lutic, B. Coq, R. Durand and R. Teissier, *J. Catal.*, 2003, **219**, 167-175.
- 37 M. Mokhtar, T. S. Saleh and S. N. Basahel, *J. Mol. Catal. A: Chem.*, 2012, **353-354**, 122-131.
- 38 P. Liu, M. Derchi and E. J. M. Hensen, *Appl. Catal. B: Environ.*, 2014, **144**, 135-143.
- 39 D. F. Wang, X. L. Zhang, W. Wei and Y. H. Sun, *Catal. Commun.*, 2012, **28**, 159-162.
- 40 D. F. Wang, X. L. Zhang, Ch. L. Liu, T. T. Cheng, W. Wei and Y. H. Sun, *Appl. Catal. A: Gen.*, 2015, DOI: 10.1016/j.apcata.2015.04.034.
- 41 G. D. Wu, X. Wang, B. Chen, J. P. Li, N. Zhao, W. Wei and Y. H. Sun, *Appl. Catal. A: Gen.*, 2007, **329**, 106-111.
- 42 P. Unnikrishnan and D. Srinivas, *Ind. Eng. Chem. Res.*, 2012, **51**, 6356-6363.
- 43 R. Bírjega, O. D. Pavel, G. Costentin, M. Che and E. Angelescu, *Appl. Catal. A: Gen.*, 2005, **288**, 185-193.
- 44 E. Rodrigues, P. Pereira, T. Martins, F. Vargas, T. Scheller, J. Correa, J. Del Nero, S. G. C. Moreira, W. Ertel-Ingrisch, C. P. D. Campos and A. Gigler, *Mater. Lett.*, 2012, **78**, 195-198.
- 45 R. D. Shannon, *Acta Crystallogr. A*, 1976, **32**, 751-767.
- 46 M. Behrens, I. Kasatkin, S. Kuhl and G. Weinberg, *Chem. Mater.*, 2010, **22**, 386-397.
- 47 W. Yang, Y. Kim, P. K. T. Liu, M. Sahimi and T. T. Tsotsis, *Chem. Eng. Sci.*, 2002, **57**, 2945-2953.
- 48 J. P. Ramirez, J. Overijnder, F. Kapteijin and J. A. Moulijn, *Appl. Catal. B: Environ.*, 1999, **23**, 59-72.
- 49 H. G. Li, X. Jiao, L. Li, N. Zhao, F. K. Xiao, W. Wei, Y. H. Sun and B. Sh. Zhang, *Catal. Sci. Technol.*, 2015, **5**, 989-1005.
- 50 Q. X. Ma, T. Sh. Zhao, D. Wang, W. Q. Niu, P. Lv and N. Tsubaki, *Appl. Catal. A: Gen.*, 2013, **464-465**, 142-148.
- 51 H. A. Prescott, Z. Li, E. Kemnitz, A. Trunschke, J. Deutsch, H. Lieske and A. Auroux, *J. Catal.*, 2005, **234**, 119-130.
- 52 L. C. Meher, R. Gopinath, S. N. Naik and A. K. Dalai, *Ind. Eng. Chem. Res.*, 2009, **48**, 1840-1846.
- 53 D. G. Cantrell, L. J. Gillie, A. F. Lee and K. Wilson, *Appl. Catal. A: Gen.*, 2005, **287**, 183-190.
- 54 K. Tanabe, M. Misono, Y. Ono and H. Hattori, *New solid acids and bases Studies in the surface science and catalysis*, Elsevier, Amsterdam, 1989, pp. 14-16.
- 55 Z. Liu, J. A. Cortés-concepción, M. Mustian and M. D. Amiridis, *Appl. Catal. A: Gen.*, 2006, **302**, 232-236.
- 56 G. D. Wu, X. L. Wang, W. Wei and Y. H. Sun, *Appl. Catal. A: Gen.*, 2010, **377**, 107-113.
- 57 Y. Ch. Fu, H. Y. Zhu and J. Y. Shen, *Thermochim. Acta*, 2005, **434**, 88-92.
- 58 M. Selva, M. Fabris and A. Perosa, *Green Chem.*, 2011, **13**, 863-872.
- 59 J. C. Carter and J. E. Devia, *Spectrochim. Acta. Part A*, 1973, **29**, 623-632.
- 60 F. J. Li, H. Q. Li, L. G. Wang, P. He and Y. Cao, *Catal. Sci. Technol.*, 2015, **5**, 1021-1034.
- 61 S. K. Sahni, *Transition Met. Chem.*, 1979, **4**, 73-76.
- 62 W. Zhang, H. Wang, W. Wei and Y. H. Sun, *J. Mol. Catal. A: Chem.*, 2005, **231**, 83-88.
- 63 T. Beutel, *J. Chem. Soc., Faraday Trans.*, 1998, **94**, 985-993.

Table 1 Textural, chemical properties, and weight loss (occurring in the second and third steps of thermal decomposition) of the HTI precursors.

Samples	Mg ²⁺ :Al ³⁺ :La ³⁺ atomic ratio ^a	Lattice parameters (Å) ^b		Weight loss (%) (second: third step)	S _{BET} (m ² /g)	Pore volume (cm ³ /g)
		<i>a</i>	<i>c</i>			
HT-0La	3:1:0	3.061	23.598	18.5: -	21	0.12
HT-2La	3:1:0.2	3.063	23.624	13.9: 7.5	33	0.16
HT-5La	3:1:0.5	3.066	23.937	12.6: 8.1	41	0.24
HT-8La	3:1:0.8	3.068	24.253	12.3: 9.7	39	0.21
HT-10La	3:1:1	3.072	24.409	11.9: 10.8	36	0.19

^a The nominal atomic ratio in the synthesis mixture.

^b Determined by XRD, $a = 2d_{110}$, $c = 3d_{003}$.

Table 2 Textural, chemical and basic properties of various catalysts

Sample	S_{BET} (m^2/g)	Pore volume (cm^3/g)	Atomic ratio in solids ^a	Surface atomic ratio ^b	Amounts of basic sites ($\mu\text{mol}/\text{g}$) and contribution ^c			
			$\text{Mg}^{2+} : \text{Al}^{3+} : \text{La}^{3+}$	$\text{Mg}^{2+} : \text{Al}^{3+} : \text{La}^{3+}$	Total	W.	M.	S.
HTC-0La	124	0.33	2.69: 1: -	2.47: 1:-	193.5	68.1 (35.2)	114.2 (59.0)	11.2 (5.8)
HTC-2La	106	0.52	2.72: 1: 0.21	2.41: 1: 0.09	223.8	60.6 (27.1)	141.5 (63.2)	21.7 (9.7)
HTC-5La	95	0.49	2.83: 1: 0.54	2.64: 1: 0.16	264.5	51.8 (19.6)	180.1 (68.1)	32.6 (12.3)
HTC-8La	84	0.45	2.85: 1: 0.88	2.66: 1: 0.28	242.4	42.0 (17.3)	152.2 (62.8)	48.2 (19.9)
HTC-10La	71	0.41	2.93: 1: 1.12	2.75: 1: 0.34	211.6	22.0 (10.4)	120.4 (56.9)	69.2 (32.7)
$\text{La}_2\text{O}_2\text{CO}_3$	28	0.16	-	-	107.7	52.6 (48.9)	31.8 (29.5)	23.3 (21.6)

^a Values measured by ICP.^b Evaluated by XPS.^c The value in parentheses was the contribution of single basic sites to the number of total basic sites

Table 3 Catalytic performance of various catalysts in the present work^a.

Entry	Catalyst	MC conversion (%)	DMC selectivity (%)	DMC yield (%)	NMMC yield (%)
1	-	4.1	63.4	2.6	0
2	HTC-0La	32.3	87.3	28.2	1.2
3	HTC-2La	41.2	84.2	34.7	2.0
4	HTC-5La	67.1	80.9	54.3	4.1
5	HTC-8La	59.5	72.6	43.2	5.7
6	HTC-10La	52.4	64.5	33.8	8.9
7	La ₂ O ₂ CO ₃	21.9	51.6	11.3	0.3

^aReaction conditions: reaction temperature, 200 °C; reaction time, 6 h; catalyst amount, 0.5 g; MC, 0.05 mol; methanol, 1.0 mol. The product selectivity and yields were based on MC.

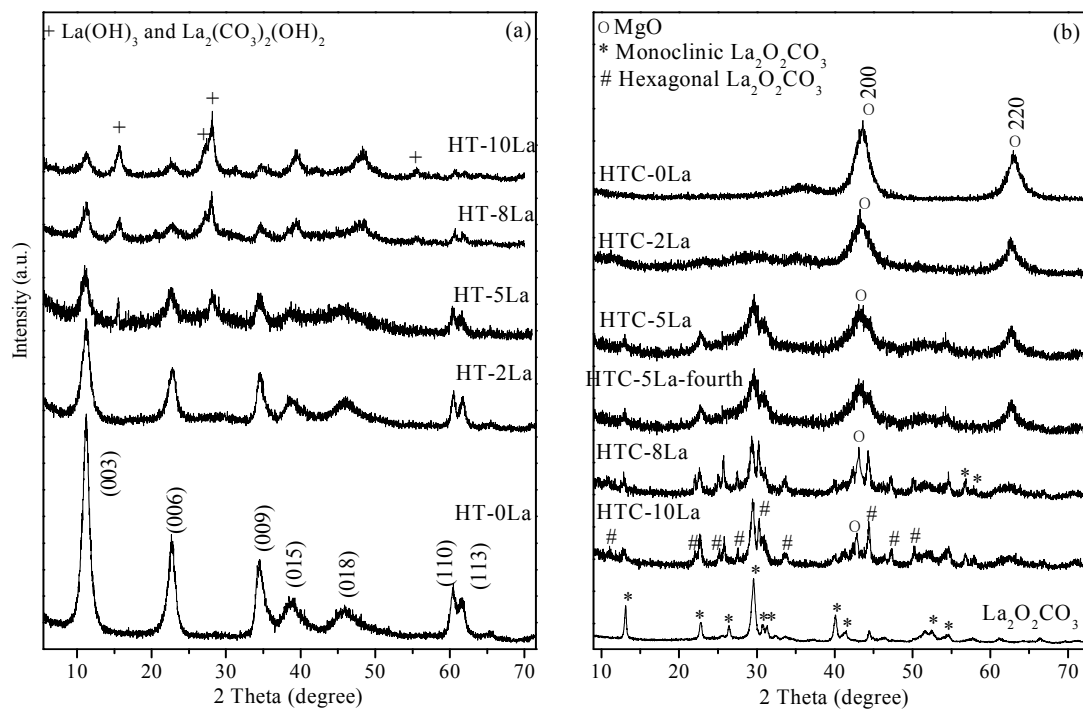


Fig. 1 XRD patterns of HT-La precursors with different La content (a); HTC-La mixed oxides with different La content and $\text{La}_2\text{O}_2\text{CO}_3$ catalysts (b).

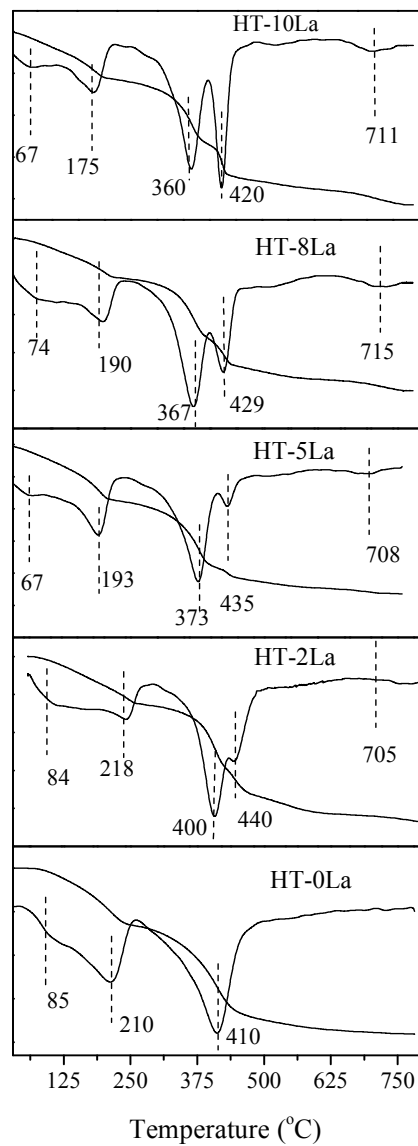


Fig.2 Thermogravimetry and differential thermogravimetry (TG-DTG) profiles of HTI precursors.

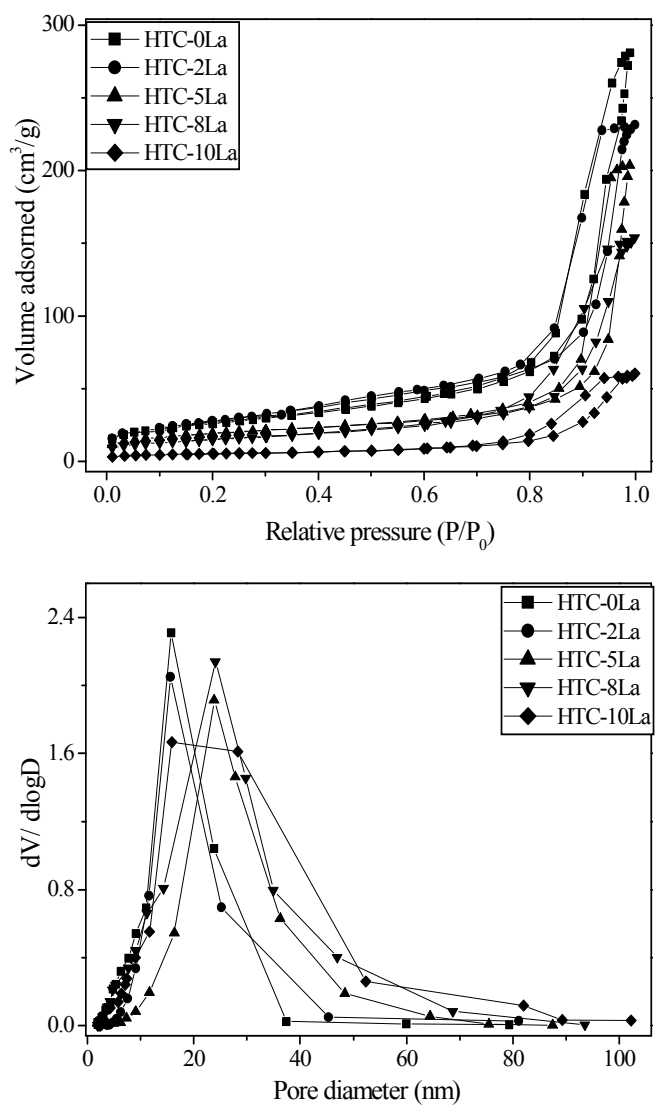


Fig.3 N_2 adsorption–desorption isotherms (a) and pore-size distributions (b) of HTC-La catalysts.

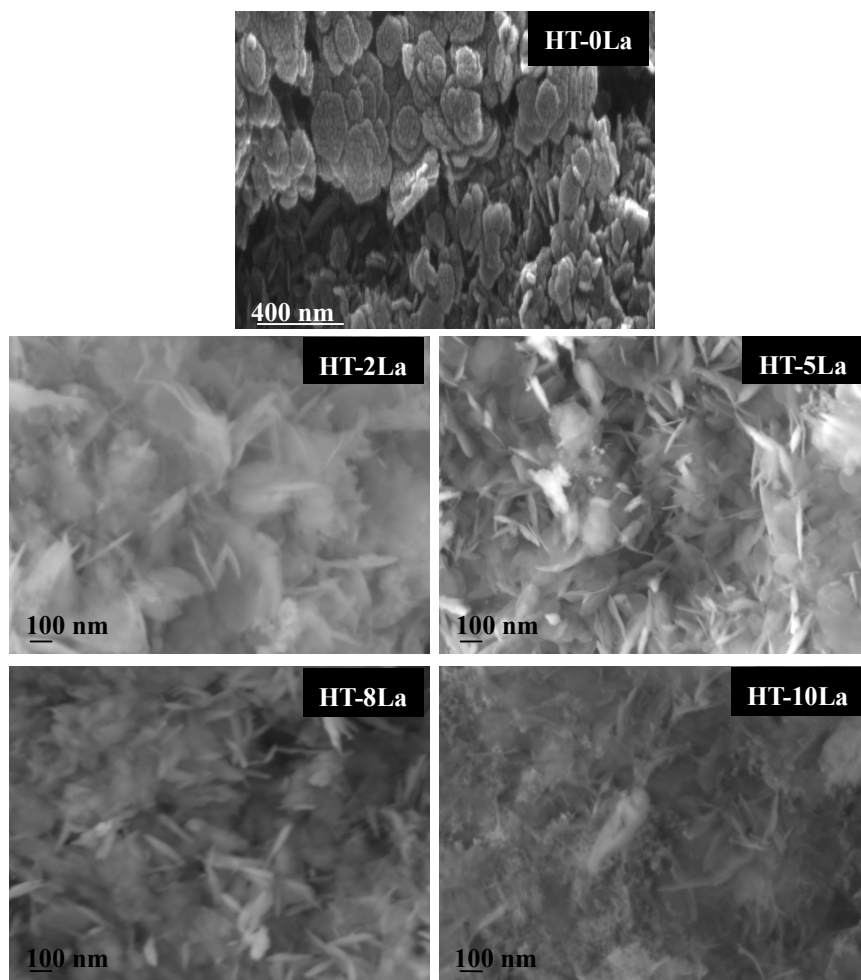


Fig. 4 SEM images of HTI precursors.

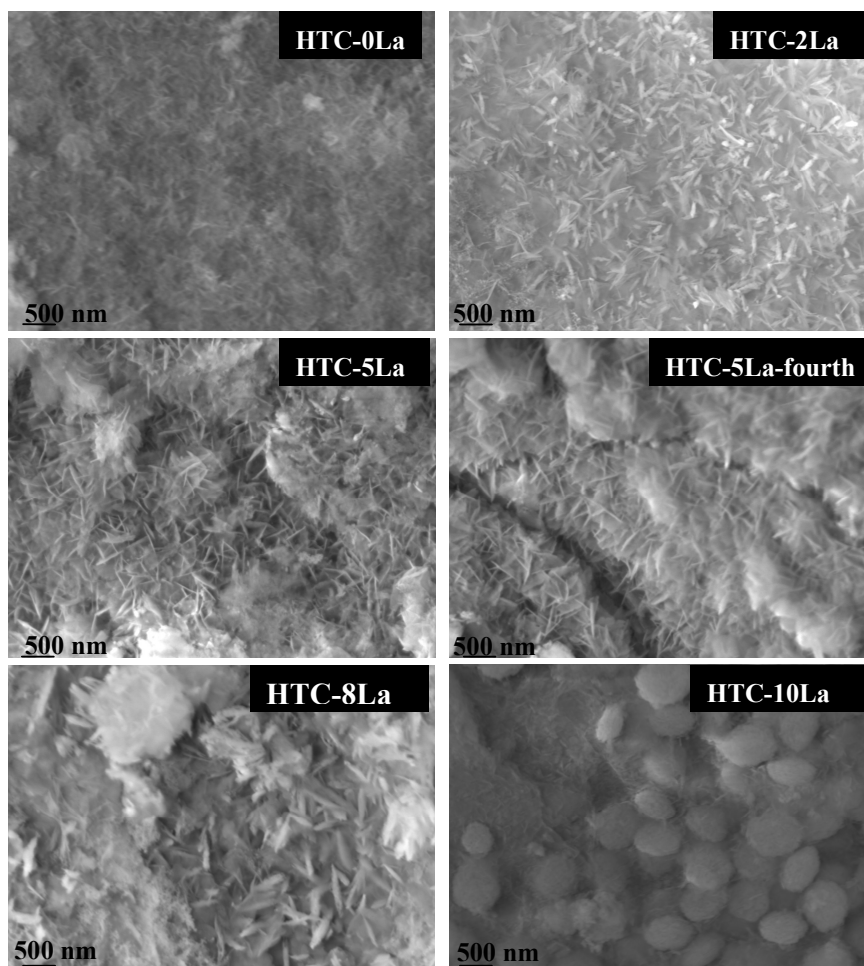


Fig. 5 SEM images of mixed oxides.

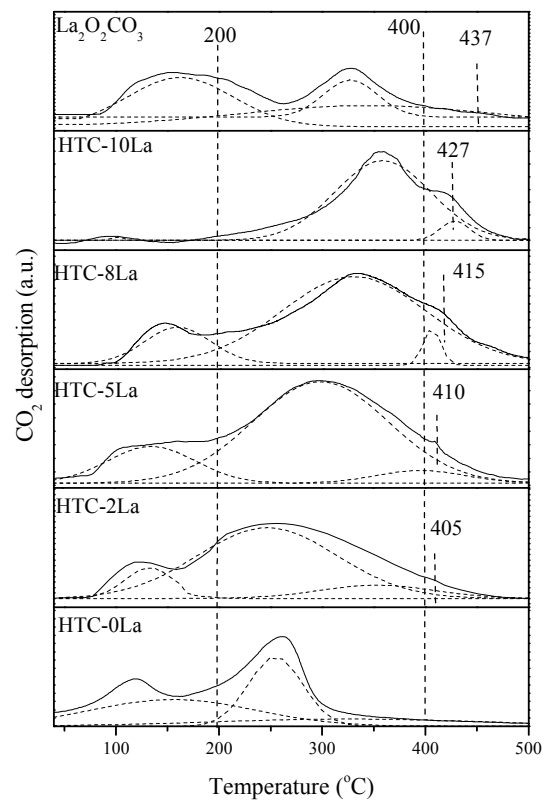


Fig. 6 CO₂-TPD of HTC-La catalysts and La₂O₂CO₃ sample.

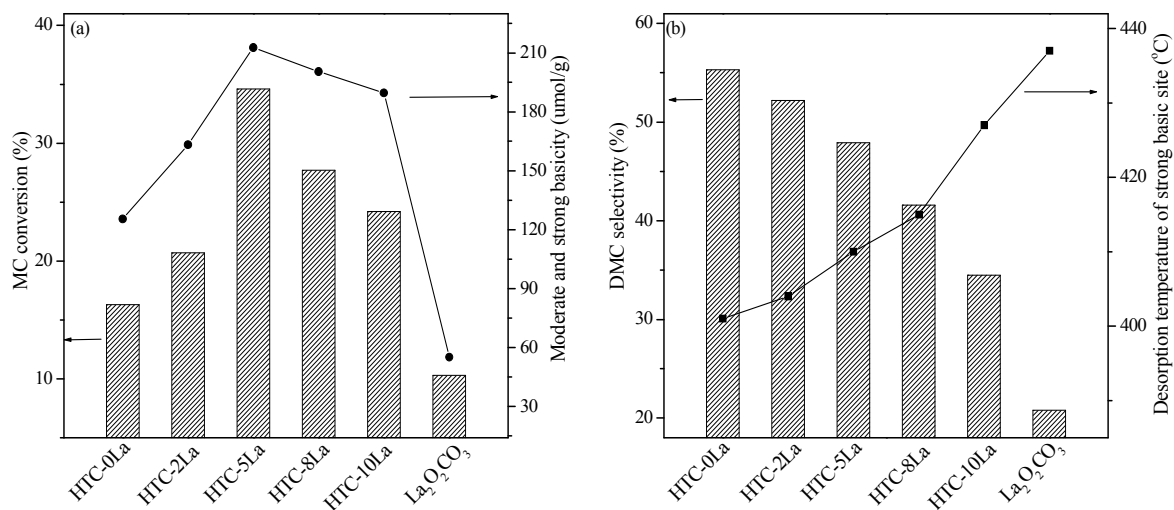


Fig. 7 The correlation between MC conversion and the amounts of both moderate and strong basic sites (a); the relationship between DMC selectivity and desorption temperature of strong basic sites (basic strength) (b).

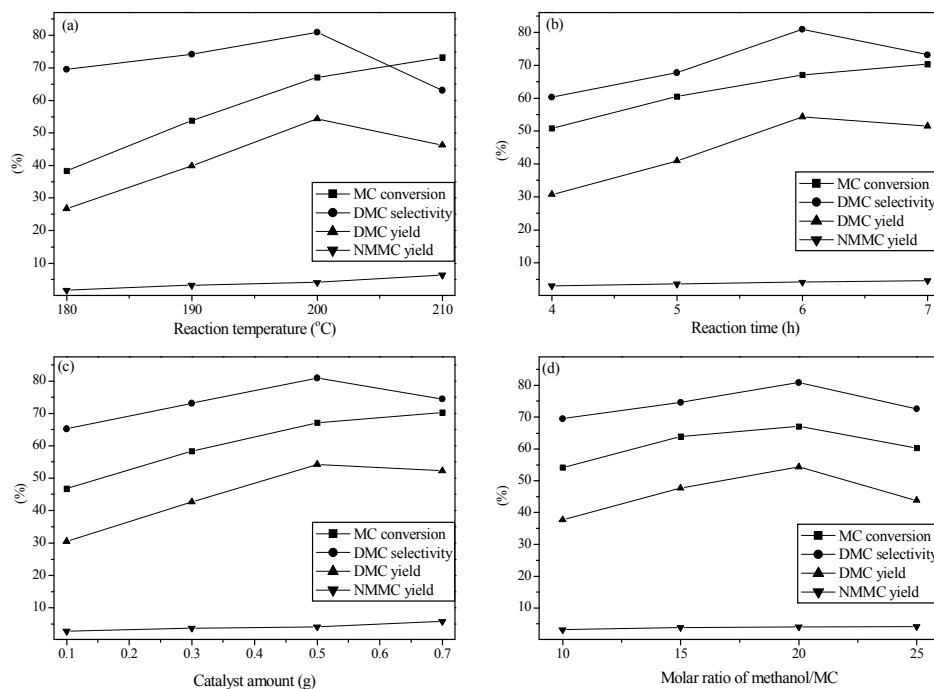


Fig. 8 Effect of reaction conditions on the DMC synthesis over HTC-5La catalyst. Effect of reaction temperature (a). Reaction conditions: reaction time, 6 h; catalyst amount, 0.5 g; molar ratio of methanol/MC, 20:1. Effect of reaction time (b). Reaction conditions: reaction temperature, 200 °C; catalyst amount, 0.5 g; molar ratio of methanol/MC, 20:1. Effect of catalyst amount (c). Reaction conditions: reaction temperature, 200 °C; reaction time, 6 h; molar ratio of methanol/MC, 20:1. Effect of molar ratio of methanol/MC (d). Reaction conditions: reaction temperature, 200 °C; reaction time, 6 h; catalyst amount, 0.5 g.

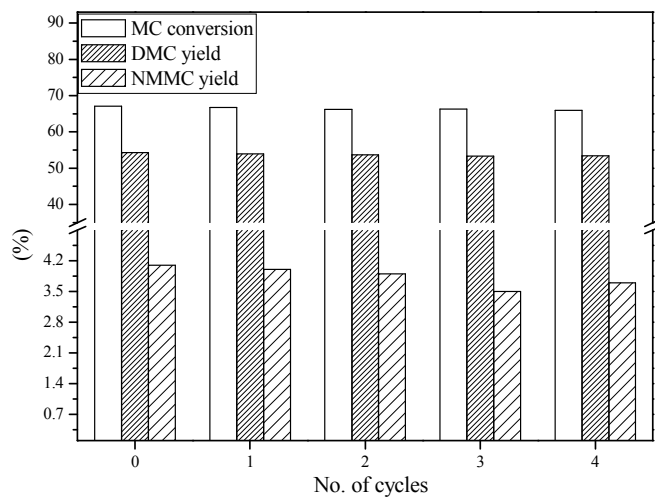


Fig. 9 Reusability of the HTC-5La catalyst for the DMC synthesis from MC and methanol. Reaction conditions: 200 °C, 6 h, 0.5 g catalyst, 0.05 mol MC, 1.0 mol methanol.

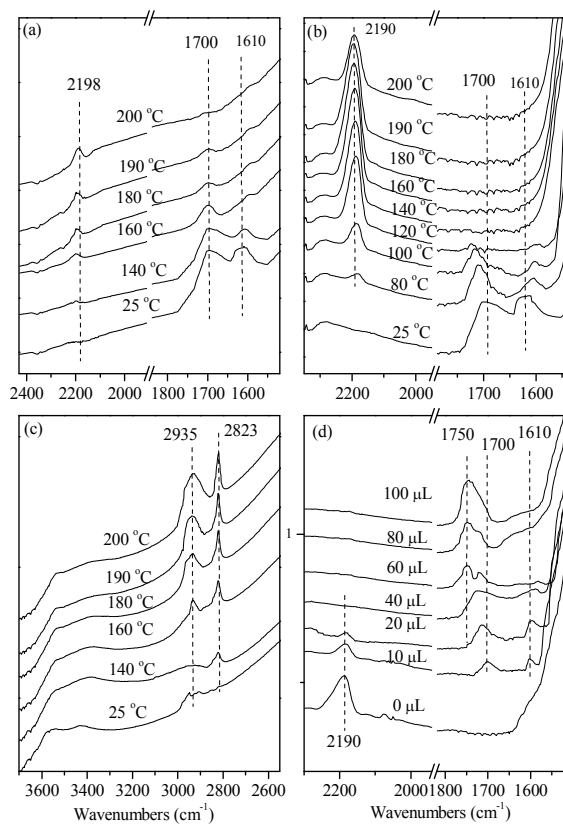
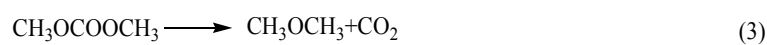
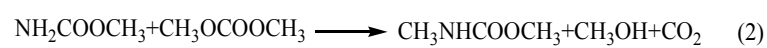
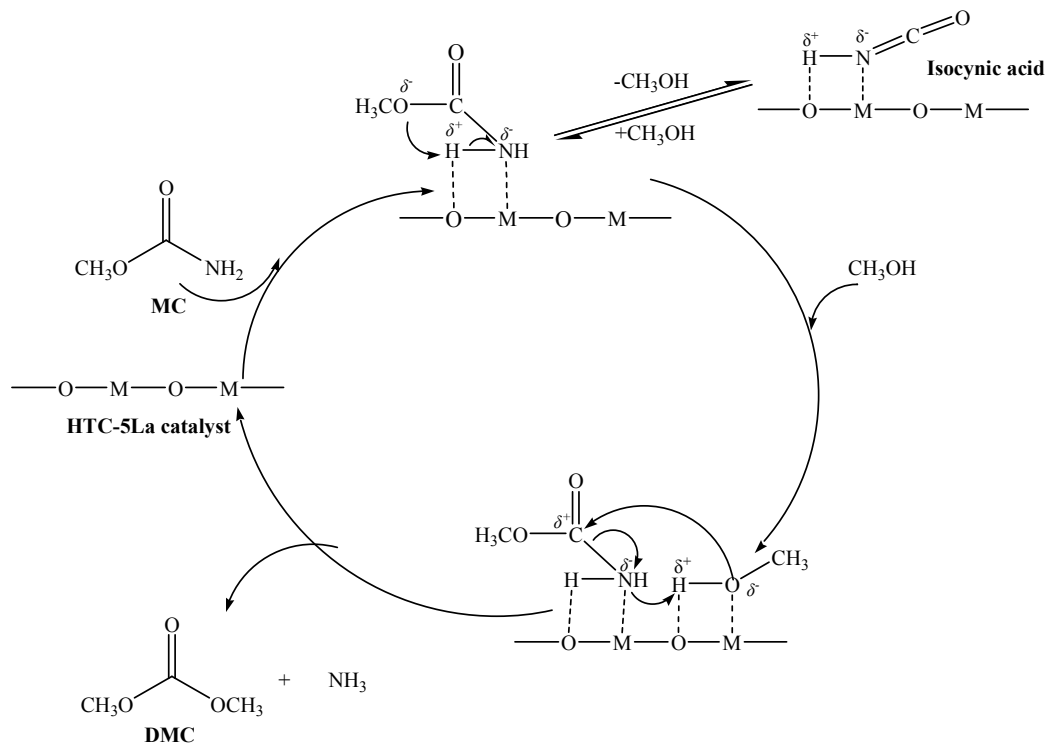


Fig.10 FTIR spectra evolution of MC (a); MC adsorbed on HTC-5La (b); methanol adsorbed on HTC-5La (c) at different temperatures; and MC with various amounts of methanol co-adsorbed on HTC-5La at 180 °C (d).



Scheme 1 The reaction system for the reaction of MC and methanol.



Scheme 2 Possible reaction mechanism for the DMC synthesis from MC and methanol over HTC-5La catalyst.

